ELSEVIER

Applied Surface Science 154–155 (2000) 627–632

applied surface science

www.elsevier.nl/locate/apsusc

Novel structure formation in poly(ethylene therephthalate) by scanning excimer laser ablation

F. Wagner, P. Hoffmann *

Institute of Applied Optics, Swiss Federal Institute of Technology Lausanne, Micro-Engineering Building, CH-1015 Lausanne EPFL, Switzerland

Received 1 June 1999; accepted 23 August 1999

Abstract

Multiple pulse laser ablation of biaxially stretched poly(ethylene therephthalate) (PET) was performed in air with a standard ArF excimer laser (193 nm) to produce micro channels. ''Scanning ablation'', with the sample moving during irradiation, was extensively studied. A new type of surface structure on the channel floor was obtained. The channel floor originates from irradiation of the ramp at the end of the channel. Three structure types were observed on ablated ramps. Each of these structures occurs within a certain range of ramp angles. The angle of incident light is not responsible for the structural changes, which is in agreement with the literature. Other possible mechanisms, such as the influence of the sample geometry near the irradiated area influencing the structure formed on the ablated surface, are discussed.

Keywords: Structure formation; Surface modification; PET; Scanning ablation

1. Introduction

A large number of articles about polymer ablation with excimer lasers have appeared since the first results obtained by Srinivasan and Mayne-Banton in 1982 [1]. The major topic in this area is the ablation rate of different polymers with various fluence ranges, wavelengths, and pulse lengths. Another topic of interest is the surface structure and the chemical composition that results from ablation [2].

Several types of polymer ablated surface structures are reported in the literature. For poly(ethylene therephthalate) (PET), three classes of structures are known. First, at fluences below the ablation threshold, a periodic pattern with a period close to the irradiation wavelength develops within a small fluence range (3–5 mJ/cm^2 for irradiation at 193 nm). These kind of structures are often referred to as light-induced periodic surface structure (LIPSS) [3]. Second, at fluences around the ablation threshold, dendrite-like structures develop when the irradiation is carried out in vacuum [4,5].

Finally, for fluences well above the ablation threshold, a nap or wall type structure develops in stretched PET foils [1,6,7]. This type of structure gets more pronounced with an increase in fluence and number of pulses. Our experiments were all carried out at fluences well above the ablation

* Corresponding author. Tel.: +41-21-693-60-18; fax: +41-21-693-37-01.

E-mail address: patrik.hoffmann@epfl.ch (P. Hoffmann).

PII: S0169-4332(99)00467-5

threshold. In order to distinguish this known type of structure from the ones that we observed only in scanning ablation experiments, we named it the ''static structure''.

A detailed investigation of the static structure was given by Hopp et al. [8]. Among other effects, they examined the structure changes occurring by variation of the angle of incidence of the light. They found that the polygon borders separating the naps became longer in the direction of the incident light when the angle of light incidence exceeded 70°. For angles below 70°, only minor structural changes were observed.

In scanning ablation, we also irradiate a surface under an angle. The difference is that in our case, we observed an important structural change already at angles bigger than 11°. We repeated the experiment of Hopp et al. [8] at an angle of 45° and could not observe a structural change, i.e., we confirmed the results of Hopp et al. [8]. As consequence, we need to study the microscopic differences between these two experiments.

In this article, we show that scanning ablation leads to two new types of surface structures — ''scanning structure'' and ''smooth structure'' — in a certain parameter range. Furthermore, we present the results that we obtained up to now on the structural change between static and scanning structures.

2. Experimental

The samples were 100 μm thick, and composed of commercial PET [Melinex, type S, ICI]. The samples were usually exposed to 200 pulses of about 20 ns duration at 193 nm [LPX 205 Excimer Laser, Lambda Physik]. The repetition rate of the pulses varied between 1 and 50 Hz and the investigated fluence range covered 75–1200 mJ/cm^2, i.e., well above the measured ablation threshold of 36 mJ/cm^2. The experimental setup is a standard ablation setup consisting of an excimer laser, a variable attenuator [Excitech], a beam homogenizer [Excitech], and a mask that is imaged at 10 × demagnification on the sample by a refractive objective [Excitech]. For channel production, the sample is mounted on a high-precision stepper-motor translation stage [Microcontrole]. The minimum step size of the translation stage (0.1 μm) is well below the resolution of the optical projection system (≈ 3 μm). The ablated surface structure was investigated by field emission secondary electron microscopy (FESEM), [Philips XL 30 FE] at 1 kV acceleration voltage without conductive coating.

If one considers that for any ablation experiment the fluence on the sample is limited by the available laser power, it is clear that only a very small area can be illuminated with each pulse. In order to obtain channels longer than this maximally illuminated area, the following two ''modes'' of ablation were applied.

(a) In the ''static ablation'' mode, we used a rectangular mask of 400 μm × 10 mm to drill a hole 40 μm in width and 1000 μm in length. The sample was then moved 1000 μm along the long axis, and the next hole was drilled just next to the first one. This procedure was repeated.

(b) In the ''scanning mode'', we also used a rectangular mask to illuminate an area of width 40 μm and length equal to the effective mask length, a (ranging from 50 μm to 1 mm), but we moved the sample during the illumination in the direction of a.

In both modes, the depth of the channels, $d_{tot} = n \times h(\Phi)$, depends on the number of pulses, n, that reach the same position on the sample and the ablation rate per pulse, $h(\Phi)$, at a fluence, Φ. In static ablation, n is simply the number of pulses that are used between sample movements. In scanning ablation, n is given by $n = fa/v$. Here, f is the pulse repetition rate of the laser, v is the scanning velocity of the sample, and a is the effective mask length. Usually, we use $n = 200$ which results at 1200 mJ/cm^2 in channels having a cross-section of about 40×40 μm^2.

3. Results

3.1. Channel geometry and parameters of scanning ablation

In multiple pulse scanning ablation, theoretically, the irradiated area has the shape of a stairway. Fresh material is fed to the beam at the top of the stairway and used material leaves the irradiated zone at the bottom. The total length of the stairway equals the

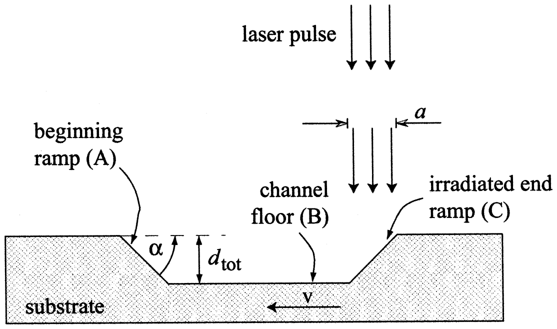

Fig. 1. Channel production by scanning ablation: the schematic shows a cross section of the channel along the channel direction. The sample moves from right to left.

effective mask length, a. The total depth of the stairway corresponds to the depth of the channel. The step width of the stairway equals the distance by which the substrate is moved between two subsequent laser pulses and the step height is given by the ablation rate per pulse, $h(\Phi)$. If, as in our case, the step width is smaller than the resolution of the optical system, the stairway becomes simply a ramp. Its angle, α, is given by $\tan(\alpha) = d_{tot}/a$ (Fig. 1).

The material that is moved out of the irradiated zone before the first n laser pulses are fired, also forms a ramp. During channel production, this ramp is not irradiated. We define this ramp as the beginning of the channel and the irradiated ramp as the end of the channel (Fig. 1).

3.2. Structure on the channel floor

On the channel floor, we observed the well-known ''static structure'' (Fig. 2a and b) as described earlier [7,8] even after scanning ablation with long masks and low fluences. The formation of this structure can be attributed to stresses in the material that are caused by the fabrication process [9]. As a result, the main orientation of the structure is given by the

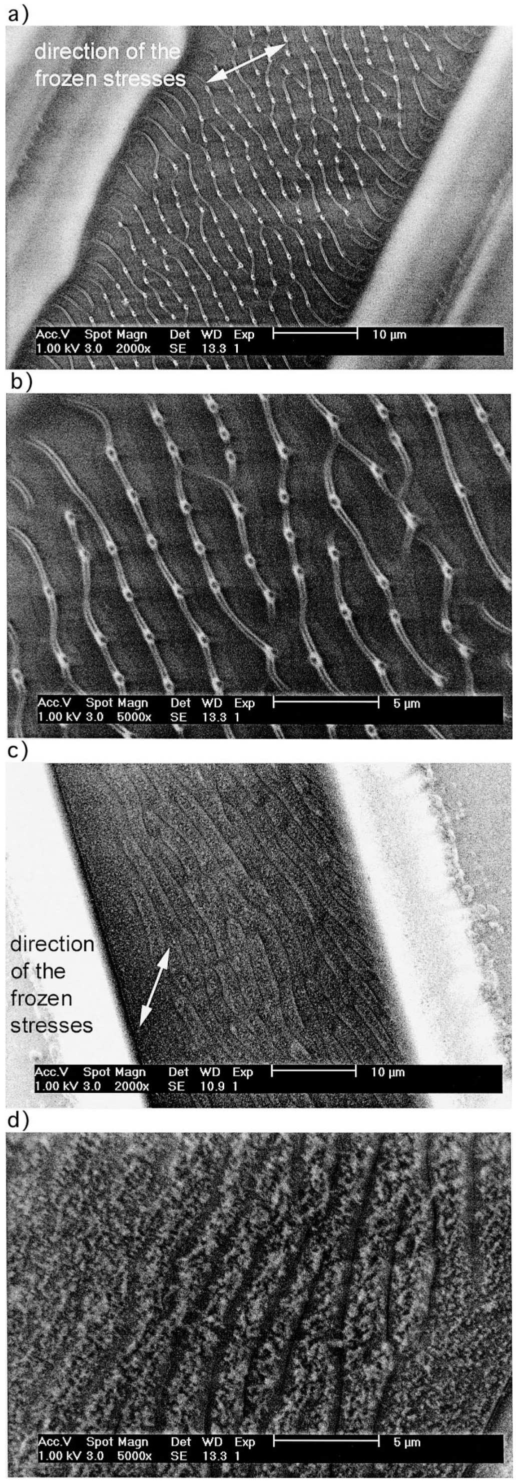

Fig. 2. FESEM micrographs of the channel floor at two different magnifications. (a) and (b) show ''static structures'' whereas (c) and (d) show ''scanning structures''. Fluences were equal in (a) and (c), ($\Phi = 600$ mJ/cm^2) and in (b) and (d) ($\Phi = 1200$ mJ/cm^2). All channels were made with the same number of pulses, $n = 200$. The scanning structure may contain redeposited materials (debris) (d).

orientation of the sample and not by the direction of the channel (Fig. 2a and b).

However, in scanning ablation with higher fluences or shorter mask lengths [10], we observed the new structure shown in Fig. 2c and d. The principal orientation of this structure is given by the direction of the channel. This result means that stresses in the material do not contribute significantly to its formation, as is the case for static structures.

Besides the effective mask length, a, and the fluence, Φ, the pulse repetition rate, f, and the scanning velocity, v, are also parameters of scanning ablation. With our 100-μm-thick samples, we observed only a negligible influence by the repetition rate, f, on the structures formed in the range of 1 to 50 Hz, both for static and scanning structures. The scanning velocities applied in our experiments ($v <$ 250 μm/s) are negligible compared to the velocities of the ejected particles at the applied fluences (0.2–10 km/s [11,12]). Therefore, the influence of the scanning velocity on the structure is negligible. This assertion was confirmed by an experiment where the scanning structure was obtained without scanning the sample (see Section 3.3). Hence, the mask length, a, and the fluence, Φ, are the most important parameters.

If we observe closely the structure of the channel floor in static ablation (Fig. 2a), we see that near the walls, the structure is always perpendicular to them. This zone is about 3 μm wide, which corresponds very well with the optical resolution of our mask projection. At the border, there is a decrease in the fluence, that reaches the substrate and as consequence, a rounded corner forms between the channel floor and the walls. In this inclined region, we always see a change in the structural orientation similar to what we observe for ablated ramps (see below).

3.3. Structure formation on ramps

As already mentioned in Section 3.1, only the end ramp is irradiated in scanning ablation. This fact means that the processes on this ramp determine the structure on the channel floor. An investigation of 30 samples revealed that the channel floor (B) and the end ramp (C) always showed approximately the same structure (see example in Fig. 3a). However, at high fluences and short mask lengths, we observed a different structure on the ramps, which was not observed on the channel floor. Under these condi-

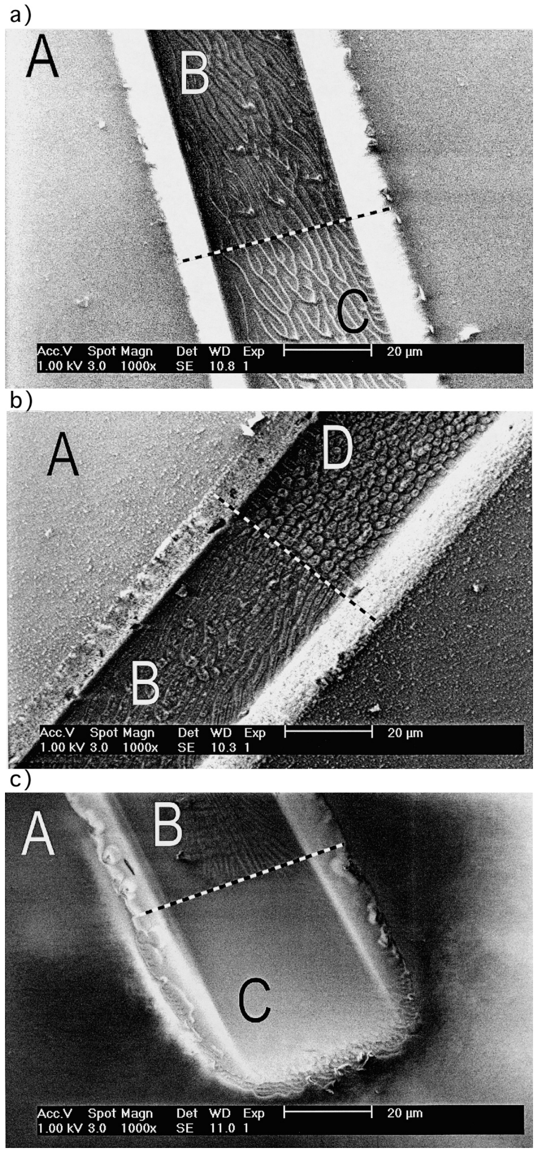

Fig. 3. Beginning (b) and end (a) of the same channel. Parameters: $a = 100$ μm, $n = 200$, $\Phi = 600$ mJ/cm^2 ($f = 50$ Hz, $v = 25$ μm/s). A smooth end ramp of a channel made with $a = 50$ μm, $n = 200$ and $\Phi = 600$ mJ/cm^2 is shown in (c). The different regions of the micrographs are designed with: A for the non irradiated flat sample surface, B for the channel floor, C for the end ramp, and D for the beginning ramp.

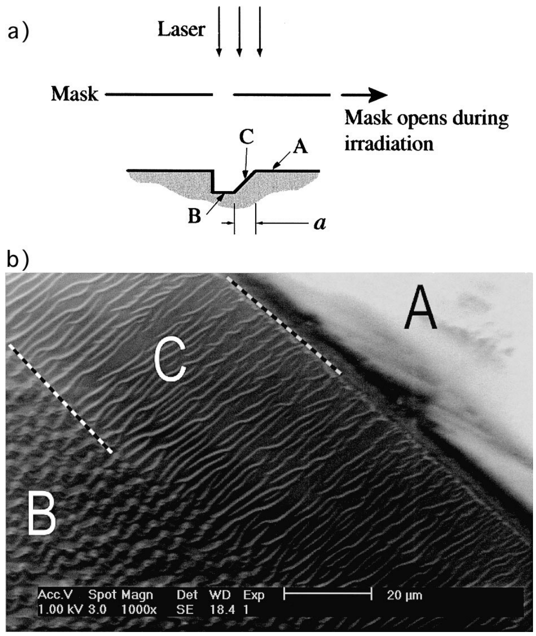

Fig. 4. (a) Illustration of the ramp production without scanning of the substrate. (b) FESEM micrograph showing a ramp (C) ablated with this scheme at $a = 50$ µm, $n = 200$, $\Phi = 290$ mJ/cm^2, ($f = 50$ Hz) which resulted in the ''scanning structure''.

tions, the end ramp becomes completely smooth as observed by FESEM (Fig. 3c).

The structure on the beginning ramp was that of the static type in all the observed cases, but may be covered by an important amount of redeposited material, as shown in Fig. 3b, region D. We never observed debris on the end ramp or close to it, but, further away in the channel, the debris may cover completely the principal surface structure due to a ''self-PLD'' effect [10].

Another way of producing the scanning structure is to keep the substrate fixed and move one edge of a free standing molybdenum mask during irradiation (Fig. 4a). The structure on the resulting ramps is similar to that of the end ramps in scanning ablation. Also, the change from ''static structure'' to ''scanning structure'' (Fig. 4b). occurs at the same values for a and Φ as in ''scanning ablation''. This fact further proves that the scanning velocity is not an important parameter for the structure change. The structure change occurred also when we produced a ramp without the flat part (B) representing the channel floor.

Fig. 5 summarizes the results of the structural changes on the ramps produced with the two methods. It shows the results obtained by SEM for the parameter space, which is built by the mask length, a, and the fluence, Φ. Because a certain ramp angle, α, was obtained with 200 pulses by using different pairs of a and Φ, one also finds iso-α-lines in this figure. These lines were calculated with a logarithmic expression for the ablation rate, $h(\Phi)$, i.e., $h(\Phi) = 0.0554\ln(\Phi) - 0.1983$, which was fit to

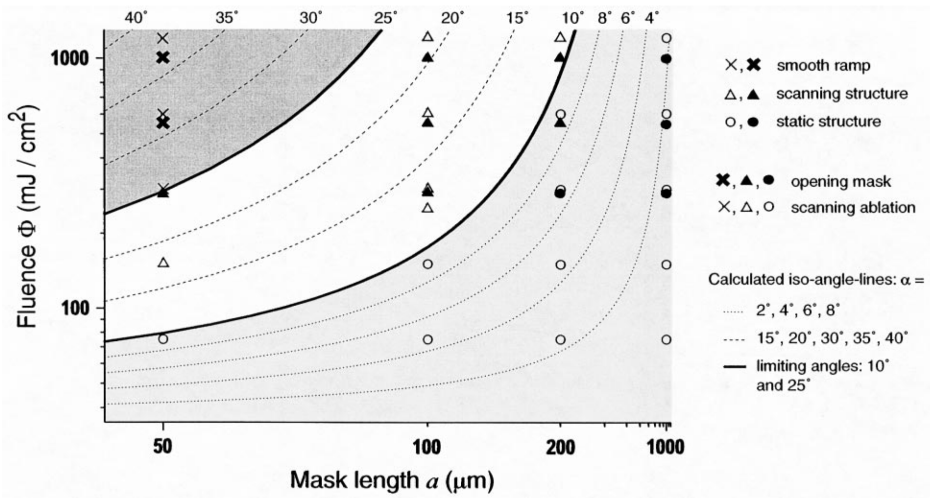

Fig. 5. Schematic diagram depicting three different zones of surface structure obtained by excimer laser ablation of PET. Ramp angles above 25° result in smooth surfaces. For further explanations, see text.

measured profilometer data. The angle, α, for a pair of values a and Φ is then calculated by $\tan(\alpha) = n \times h(\Phi)/a$ (at $n = 200$).

We find that the obtained structures separate nearly perfectly into three regions which are limited by the iso-angle-lines of the ''limiting angles'', α_1. The static structure is separated from the scanning structure by $\alpha_1 = 10°(\pm 0.5°)$, whereas the scanning structure transforms to smooth ramps at $\alpha_1 = 25°(\pm 0.5°)$. This finding means that, for example, if we want to have a smooth structure on the ramp, we need a ramp angle of more than 25°. Our investigations still continue and it is not yet clear if the values of the ''limiting angles'' depend on the strength of the stresses in the sample, on the pressure of the gas environment, on the sample material, or on other parameters.

4. Discussion

When we compared the data presented in this article with the data of Hopp et al. [8], we noticed that we address the fundamental question: In which system can we describe structure formation during ablation? We ask this question because the system usually used, which consists of light, the material properties of the irradiated surface, and a gas environment, is the same in both experiments. We suggest that the neighborhood of the irradiated surface play an important role in the formation of the scanning structure.

The phenomenon that the ramp angles, α, fall into three distinct ranges which produce three structure types on the ramps indicates that the asymmetry of the nearby surfaces with respect to the normal of the irradiated area is important. Up to now; it is not clear how this asymmetry could influence the structure formation. Shock waves either in the atmosphere or in the substrate itself, as well as, a difference in surface tension occurring in the liquid layer may be valuable explanations. None of these hypotheses has been proven, but it is clear that a lateral temperature gradient, which might be present on the ramp at $f = 50$ Hz, does not affect the structural change on the basis of the results from the control experiment at low repetition rate ($f = 1$ Hz).

5. Summary and conclusion

We presented new surface structures, called ''scanning structures'', which were observed after scanning ablation of stretched PET foils. Further more, we investigated the influence of the mask length, a, fluence, Φ, pulse repetition rate, f, and scanning velocity, v, on the structure change for the static and scanning structure. We showed that the structural change that occurred on the ramps was the origin of the structural change on the channel floor. Because all ramps with ''static structure'' occur for angles $\alpha < 10°$, all ramps with ''scanning structure'' occur for angles of $10° < \alpha < 25°$ and all ramps produced with angles of $\alpha > 25°$ are smooth, the angle, α, may serve as an important parameter for characterizing the structural change. In conclusion, the geometric arrangement of the sample near the ablated region seems to influence the structural formation on the ablated surface. However, up to now, it is not clear whether the ramp angle is the determining parameter, and how the environment can influence the structure formation.

Acknowledgements

We thank James Derose for the critical revision reading of this article.

References

[1] R. Srinivasan, V. Mayne-Banton, Appl. Phys. Lett. 41 (1982) 576.
[2] S. Lazare, R. Srinivasan, J. Phys. Chem. 90 (1986) 2124.
[3] M. Csete, Z. Bor, Appl. Surf. Sci. 133 (1998) 5.
[4] J. Heitz, E. Arenholz, D. Bäuerle, H. Hibst, A. Hagemeyer, G. Cox, Appl. Phys. A 56 (1993) 329.
[5] J. Heitz, E. Arenholz, D. Bäuerle, K. Schilcher, Appl. Surf. Sci. 81 (1994) 103.
[6] L. Wefers, D. Bosbach, W. Rammensee, E. Schollmeyer, Appl. Surf. Sci. 69 (1992) 418.
[7] T. Bahners, W. Kesting, E. Schollmeyer, Appl. Surf. Sci. 69 (1993) 12.
[8] B. Hopp, M. Csete, K. Révész, J. Vinko, Z. Bor, Appl. Surf. Sci. 96–98 (1996) 611.
[9] E. Arenholz, V. Svorcik, T. Kefer, J. Heitz, D. Bäuerle, Appl. Phys. A 53 (1991) 330.
[10] F. Wagner, P. Hoffmann, Appl. Phys. A 69 (1999), in press.
[11] R. Kelly, A. Miotello, B. Braren, C.E. Otis, Appl. Phys. Lett. 60 (1992) 2980.
[12] P.E. Dyer, J. Sidhu, J. Appl. Phys. 64 (1988) 4657.